Chapter 24

The SCM Concept and Creation of ARM Forcing Datasets

MINGHUA ZHANG

State University of New York at Stony Brook, Stony Brook, New York

RICHARD C. J. SOMERVILLE

Scripps Institution of Oceanography, University of California, San Diego, La Jolla, California

SHAOCHENG XIE

Lawrence Livermore National Laboratory, Livermore, California

1. The concept of SCM for ARM

Two papers published in the early 1990s significantly influenced the subsequent design of ARM and its adoption of the single-column model (SCM) approach. The first paper, by Cess et al. (1990), showed a threefold difference in the sensitivity of climate models in a surrogate climate change that is attributed largely to cloud–climate feedbacks. The second paper, by Ellingson et al. (1991), reported 10%–20% difference in the calculated broadband radiation budget and 30%–40% difference in the radiative forcing of greenhouse gases in the radiation codes of climate models. At that time, the U.S. Department of Energy (DOE) had a program to study the climate impact of the increasing amount of carbon dioxide in the atmosphere. Results from these two papers pointed to the major uncertainties in climate forcing and feedbacks of climate models.

Radiation and clouds, therefore, emerged as a focus in the DOE ARM Program to improve models. To simulate clouds, information is needed about the atmospheric dynamics beyond the vertical profiles of atmospheric thermodynamics and winds at a single station. By the early 1990s, analyses of observed atmospheric dynamics from the 1974 Global Atmosphere Research Experiment (GARP) Atlantic Tropical Experiment (GATE) had been completed (e.g., Ooyama 1987). GATE used a well-coordinated sounding array to derive the atmospheric dynamics. It was shown to be feasible to simulate atmospheric moist processes by using observed atmospheric dynamics from a well-configured measurement array (e.g., Gregory and Rowntree 1990). The concept of using SCMs to represent a single grid box of a climate model was well suited to address the uncertainties in radiation and clouds in the models. To represent different cloud regimes in a global model, ARM decided to establish three sites: the Southern Great Plains (SGP), the Northern Slope of Alaska (NSA), and the Tropical Western Pacific (TWP) (Stokes and Schwartz 1994).

An SCM is a one-dimensional (vertical) computational model of a specific columnar region of the atmosphere. It may be thought of as being extracted from the array of such columns, which make up the atmospheric portion of a global climate model or general circulation model (GCM). In the GCM, this atmospheric model column interacts at each vertical level and at every time step with neighboring columns, providing horizontal fluxes of heat, water, and momentum to and from these neighbors. By contrast, an SCM requires these fluxes to be specified, either from model data, observations, or some combination of the two. If the fluxes are set to zero, the SCM becomes one type of a radiative–convective model (RCM). One way to think of an RCM (Ramanathan and Coakley 1978) is as a horizontally averaged GCM, with the horizontal averaging over a global domain resulting in zero horizontal flux convergence. The horizontal fluxes also can be applied to cloud-resolving models (CRMs) and large-eddy simulation (LES)

Corresponding author address: Minghua Zhang, School of Marine and Atmospheric Sciences, State University of New York, Stony Brook, 145 Endeavor Building, Stony Brook, NY 11794.
E-mail: minghua.zhang@stonybrook.edu

DOI: 10.1175/AMSMONOGRAPHS-D-15-0040.1

models, which allows CRM and LES results to be used to evaluate the SCMs, especially when the physical quantities cannot be measured observationally.

Many climate modeling research groups have developed and used SCMs as tools for parameterization development. ARM has historically been a significant source of support to the small community of SCM modelers by providing research grants, observational data, and computational resources. In particular, observational data from the ARM SGP site have been a major stimulus to the development and use of SCMs because of the wealth of available measurements. The ARM's success with research involving SCMs has encouraged several modeling groups to make their own internally developed SCMs publicly available, sometimes with professionally programmed and well-documented codes. The National Center for Atmospheric Research (NCAR) climate modeling group, for example, has made single-column versions of its global climate models available for many years.

A great deal of experience has been gained in using SCMs with ARM data, and, over time, the role of SCMs in climate research has been expanded and clarified. The use of SCMs clearly has a valuable place in the hierarchy of modeling approaches, which is needed to improve the realism and trustworthiness of climate models. Of course, a wide variety of techniques has long been employed to test and validate physical process parameterizations in both weather and climate models. One straightforward method is to compare the results of full three-dimensional GCM simulations, using different parameterizations, against global observations. Another is to carry out numerical weather prediction (NWP) experiments initialized with observations and to compare the effects of different parameterizations on short- and medium-range forecast skill. Both of these approaches are important. However, carrying out a carefully coordinated model parameterization intercomparison program with three-dimensional models, even when the same basic model is used as the vehicle, is time consuming and computationally intensive, especially when the parameter space is large. Because the SCM has only one space dimension (vertical), it is very fast, and it is practical to explore large segments of parameter space by making hundreds or even thousands of integrations, which is impossible with a full GCM.

2. Early studies using SCMs

The semiprognostic model of Lord (1982) and the convective adjustment tests of Betts and Miller (1986) are early examples of the idea of using a model of a single atmospheric column. In ARM, SCMs have been widely used to investigate parameterizations of cloud-radiation processes. This approach typically involves evaluating parameterizations directly against measurements from ARM field programs and using this validation to tune existing parameterizations and to guide the development of new ones. The single-column model is thus used to make the link between observations and parameterizations. Surface and satellite measurements are both used to provide an initial evaluation of the performance of the different parameterizations. The results of this evaluation are then used to develop improved cloud-precipitation schemes, and finally these schemes are tested in GCM experiments (e.g., Lee et al. 1997). An early example of using a single-column model in this way was described by Iacobellis and Somerville (1991a,b).

A major result of ARM is that SCMs have proven themselves capable of validating parameterization results directly against ARM measurements. Climatically critical observable quantities, such as cloud liquid water and downwelling surface shortwave and longwave radiation, can be both derived from SCM results and inferred from observations at the SGP site. It is safe to say that, with extensive examples of this type of research in ARM, a major step has been achieved in fulfilling the original promise of the SCM approach.

The SCM is a convenient test bed for examining many aspects of the ways in which GCMs treat subgrid physical processes. For example, Lane et al. (2000) found strong sensitivity to vertical resolution in several test integrations in which they increased the number of layers substantially. Several possibilities are raised by this result. One possibility is that the parameterizations are constructed around implicit assumptions as to how many layers are involved so that they do not generalize to arbitrary vertical resolution and converge at sufficiently small vertical grid sizes. Another possibility is that typical GCM and NWP vertical resolutions are simply inadequate for some aspects of parameterized subgrid physics, such as marine stratocumulus clouds, although they may generally be satisfactory from the viewpoint of large-scale dynamics.

The SCM approach also has been used by the Global Energy and Water Cycle Experiment (GEWEX) Cloud System Study (GCSS)/Global Atmospheric System Study (GASS) to study cloud processes in which CRMs and LES models are also used. Most of the GCSS/GASS studies employed idealized horizontal forcing data that represent certain aspects of the observations. Early GCSS SCM studies include the modeling of stratocumulus-topped boundary layer (Bechtold et al. 1996; Zhu et al. 2005), the smoke cloud case (Bretherton et al. 1999b), the Atlantic Stratocumulus Transition Experiment (ASTEX; Bretherton et al. 1999a), and the diurnal cycle of shallow cumulus over land (Lenderink et al. 2004; Guichard et al. 2004). The GCSS/GASS case studies have enriched the

SCM studies in ARM (e.g., Guichard et al. 2004; Fridlind et al. 2012; Petch et al. 2014).

3. Requirement on large-scale forcing data

In the simplest setting, the SCMs calculate the time evolution of the vertical distributions of temperature and water vapor, schematically written as follows:

$$\frac{\partial \theta_m}{\partial t} = \left(\frac{\partial \theta_m}{\partial t}\right)_{\text{phy}} - (\mathbf{V}\cdot\nabla\theta)_{\text{LS}} - \omega_{\text{LS}}\frac{\partial \theta_m}{\partial p} \quad \text{and} \quad (24\text{-}1)$$

$$\frac{\partial q_m}{\partial t} = \left(\frac{\partial q_m}{\partial t}\right)_{\text{phy}} - (\mathbf{V}\cdot\nabla q)_{\text{LS}} - \omega_{\text{LS}}\frac{\partial q_m}{\partial p}, \quad (24\text{-}2)$$

where θ and q are potential temperature and water vapor mixing ratio; subscript m denotes model values; LS stands for prescribed large-scale fields; phy represents physical parameterizations; and other symbols are as commonly used. In the vertical advection terms of Eqs. (24-1) and (24-2) (i.e., the last term on the right-hand side), the simulated profiles of θ and q are used, so the vertical advection terms retain some feedback of the simulated fields to the forcing fields. The horizontal advective tendencies $-(\mathbf{V}\cdot\nabla\boldsymbol{\theta})_{\text{LS}}$ and the vertical velocity ω_{LS} are the large-scale forcing (Randall and Cripe 1999). It is sometimes referred to as 2D forcing. In another formulation, the observed profiles of θ and q are used in the vertical advection term. Therefore $-(\mathbf{V}\cdot\nabla\boldsymbol{\theta})_{\text{LS}} - [\omega(\partial\theta/\partial p)]_{\text{LS}}$ is prescribed as the large-scale forcing, which is often referred as 3D forcing. In calculating the physical tendencies of θ_m and q_m [i.e., the first terms on the right-hand sides of Eqs. (24-1) and (24-2)], SCMs compute the clouds, convection, precipitation, radiation, and turbulent mixing that can be compared with observations.

The same forcing fields also can be applied to CRM or LES models. The CRMs and LESs simulate θ and q or sometimes their corresponding conservative variables of liquid water potential temperature and total liquid water. The forcing terms in Eqs. (24-1) and (24-2) are applied to all model grids in CRMs and LESs, but with θ_m and q_m in the vertical advection terms replaced by domain-averaged values.

The derivations of the large-scale forcing data from field measurements are subject to uncertainties that can directly impact the simulated cloud and radiation fields by the SCMs. These uncertainties originate from two sources. One is the instrument and measurement errors. The second is errors from scale aliasing, or sampling biases. Both error types depend on scales because horizontal derivatives are involved in the calculation of the horizontal fluxes. Generally speaking, the smaller the scale is, the larger the errors in the derivative fields.

If the accuracy requirements of the physical parameterization terms in Eqs. (24-1)–(24-2) are $1\,\text{K day}^{-1}$ and $1\,\text{g kg}^{-1}\,\text{day}^{-1}$, the comparable accuracy requirements on the errors of the horizontal differences of temperature ($\Delta\theta$) and humidity (Δq) over a distance Δx can be estimated as the following:

$$\mathbf{V}\cdot\nabla\theta \sim \left|u\frac{\Delta\theta}{\Delta x}\right| \le 1\,\text{K day}^{-1},$$

$$|\Delta\theta|_{\min} \le 1(\text{K day}^{-1})\frac{\Delta x}{|u|_{\max}} \quad \text{and}$$

$$\mathbf{V}\cdot\nabla q \sim \left|u\frac{\Delta q}{\Delta x}\right| \le 1\,\text{g kg}^{-1}\,\text{day}^{-1},$$

$$|\Delta q|_{\min} \le 1(\text{g kg}^{-1}\,\text{day}^{-1})\frac{\Delta x}{|u|_{\max}}.$$

Given $|u|_{\max} \sim 10\,\text{m s}^{-1}$ and over a distance of 200 km, the above inequalities require that

$$|\Delta\theta|_{\min} \le 0.23\,\text{K} \quad \text{and} \quad (24\text{-}3)$$

$$|\Delta q|_{\min} \le 0.23\,\text{g kg}^{-1}. \quad (24\text{-}4)$$

It should be emphasized that these are the relative errors across the distance of Δx. The requirement on the pressure vertical velocity error is

$$\left|\omega\frac{\partial\theta}{\partial p}\right| \le 1\,\text{K day}^{-1},$$

$$|\omega|_{\min} \le 1(\text{K day}^{-1})\frac{pg}{R_dT}\Big/\left(\frac{\partial\theta}{\partial z}\right) \approx 10\,\text{mb day}^{-1} \quad \text{or}$$

$$\left|\omega\frac{\partial q}{\partial p}\right| \le 1\,\text{g kg}^{-1}\,\text{day}^{-1},$$

$$|\omega|_{\min} \le 1(\text{g kg}^{-1}\,\text{day}^{-1})\Big/\left(\frac{\partial q}{\partial p}\right)_{\max} \approx 10\,\text{mb day}^{-1}.$$

The requirement on the difference of horizontal winds across the domain that corresponds to the above error in vertical velocity can be estimated as follows:

$$\frac{\Delta u}{\Delta x} \sim \frac{\partial\omega}{\partial p}.$$

Assuming a vertical layer of 100 hPa, we get

$$|\Delta u|_{\min} \le 0.12\,\text{m s}^{-1} \quad (24\text{-}5)$$

The error bounds of the spatial differences in Eqs. (24-3)–(24-5), corresponding to an accuracy requirement of $1\,\text{K day}^{-1}$ and $1\,\text{g kg}^{-1}\,\text{day}^{-1}$ in the forcing data, need to be scaled proportionally if the horizontal scale is different from 200 km. These magnitudes are comparable to instrument errors (Zhang and Lin 1997), but since they are relative errors across the space, the systematic instrument errors are reduced if the same equipment is

used over the domain. The random errors may be suppressed by averaging over vertical levels. The more problematic errors are those caused by scale aliasing or sampling bias. These errors are often handled by using statistical approaches. In ARM, they are dealt with additionally by using known physical constraints.

Because of the errors in the forcing data, when integrated for multiple days, the temperature and moisture errors in the SCMs can build up, leading to the drift of SCMs into a very different climate regime that is no longer useful as a diagnostic. A common practice to remedy the drift is to reinitialize the SCM to conduct short periods of integrations and then concatenate them into a multiday long period. Another practice is to weakly apply relaxation terms to the model to observed temperature and humidity, in which case the temperature and water vapor fields are no longer good measures of model performance.

4. Forcing data from field experiments prior to ARM

In the objective analysis of field experimental data of a sounding array, in theory both the horizontal advective tendencies and the large-scale vertical velocity can be obtained by using finite difference approximation of the horizontal derivatives when the input data are regularly spaced. Since balloon sounding stations are never regularly distributed, interpolations and extrapolations are needed to preprocess the atmospheric temperature, water vapor, and winds into a regular set of grids. This method is referred to as the "regular grid method" in Zhang et al. (2001). In this method, the forcing data are calculated at each grid, and area averages are performed to obtain forcing for the study domain. An alternate method is to write the advective tendencies in flux form. The horizontal flux divergence terms, when averaged over a domain, are calculated by line integrals at the lateral boundaries of the study domain. This approach is referred to as the "line-integral method."

A key element in the regular grid method is the fitting of atmospheric state variables to the desired grids. The fitting results depend on the choice of the assumed functional form, which can be quite subjective. Commonly used methods are linear fitting and the quadratic and spline fittings (Davies-Jones 1993; Thompson et al. 1979). The more convenient algorithms are the Barnes (1964) and the Cressman (1959) schemes (Lin and Johnson 1996). In these schemes, a background field (or initial guess) is used at the observational locations; the difference between the observation and the initial guess field is then interpolated to the regular set of grids to adjust the background fields at these grids. The calculation can be performed iteratively to reach the desired corrections. Both the interpolation method and the number of integrations can affect the final analysis. A more sophisticated method uses a statistical interpolation scheme, such as that of Ooyama (1987).

The line-integral method depends on the number of atmospheric measurements at the boundary of the study domain. It therefore contains fewer subjective assumptions than the regular grid method. An important requirement is that there need to be a sufficient number of measurement stations at the domain boundary. The line-integral method typically does not use measurements inside the study domain in calculating the lateral boundary fluxes.

The regular grid method is more suited to analyze data with many scattered measurement stations, while the line-integral method is more suited for a well-positioned sounding array with few measurement stations. Zhang et al. (2001) presented a hybrid approach in which the regular grid method is used to improve the lateral boundary fluxes in the line-integral method.

Both methods have been used in the past to derive SCM large-scale forcing data in field experiments. One of the most widely used legacy datasets was from the GATE in 1974. Ooyama (1987) derived the GATE objective analysis by designing a statistical regular grid method onto which a penalty function is imposed to ensure smoothness of the fields. While the GATE data by Ooyama (1987) have been used widely, a standard analysis algorithm is not available because many subjective procedures and judgments were made through trial and error tests for each data point.

Another widely used SCM forcing dataset was from the Tropical Ocean and Global Atmosphere Coupled Ocean–Atmospheric Response Experiment (TOGA COARE) from November 1992 to February 1993. Lin and Johnson (1996) used the Barnes analysis and the regular grid method to derive the forcing data. Frank et al. (1996) analyzed the TOGA COARE data using the line-integral method. The difference of the moisture budgets from these two analyses over the Intensive Flux Array (IFA) was large. The time-averaged diagnosed precipitation over the experiment period is 5.7–6.1 mm day^{-1} in Lin and Johnson (1996) and 10.5–11.8 mm day^{-1} in Frank et al. (1996). Therefore, although the analyzed data can be used to study the qualitative temporal variation of large-scale atmospheric phenomena, such as the Madden–Julian oscillation (MJO), their use to simulate the observed cloud fields for direct comparison with transient measurements of clouds can have large errors from the forcing data.

SCM forcing data have been calculated for other shorter field experiments. Many of these are in regions of Asian and Australian monsoons. They were summarized in Zhang et al. (2001). Uncertainties of the analyzed data are likely similar to those in TOGA COARE. These uncertainties represent fundamental limits of

data from the balloon sounding arrays caused by scale aliasing, as stated succinctly by Ooyama (1987, p. 2501): "To make gold, one must start with gold."

Atmospheric reanalysis or operational analysis also can be used to obtain the large-scale forcing. However, because the operational models suffer from biases of cloud and precipitation parameterizations that ARM aims to improve, these products are not always suited for SCM results to be compared with observations. For example, operational models typically cannot simulate the timing and magnitude of observed precipitation, which results in a bias in the large-scale vertical velocity in these products. Large-scale forcing in the European Center for Medium-Range Weather Forecasts (ECMWF) operational analysis and the North American Regional Reanalysis (NARR) has been evaluated in Xie et al. (2003, 2006) and Kennedy et al. (2011), and it was shown that cloud fields and vertical velocity in these products contain large errors during precipitation events.

5. The ARM variational analysis method

Recognizing the accuracy limit in large-scale forcing data and the need for transient forcing data in ARM, Zhang and Lin (1997) developed a constrained variational algorithm to incorporate more measurements to improve the SCM forcing data. Physical constraints are enforced. These constraints include column-integrated conservations of atmospheric masses of moist air and water vapor as well as heat and momentum. They are written as follows:

$$\frac{1}{g}\frac{\partial p_s}{\partial t} = -\langle \nabla \cdot \mathbf{V} \rangle ; \tag{24-6}$$

$$\frac{\partial \langle q \rangle}{\partial t} = -\langle \nabla \cdot \mathbf{V} q \rangle + E_s - \mathrm{Prec}; \tag{24-7}$$

$$\frac{\partial \langle s \rangle}{\partial t} + \langle \nabla \cdot \mathbf{V} s \rangle = R_{\mathrm{TOA}} - R_{\mathrm{SRF}} + L_v \mathrm{Prec} + \mathrm{SH} + L_v \frac{\partial \langle q_l \rangle}{\partial t}; \quad \text{and} \tag{24-8}$$

$$\frac{\partial \langle \mathbf{V} \rangle}{\partial t} + \langle \nabla \cdot \mathbf{V}\mathbf{V} \rangle + f\mathbf{k} \times \langle \mathbf{V} \rangle + \nabla \langle \phi \rangle = \boldsymbol{\tau}_s . \tag{24-9}$$

In the above equations, $\mathbf{V}$, s, and q are the atmospheric state variables of the wind vector, dry static energy, and water vapor; p_s is the surface pressure; q_l is the cloud liquid water content; and ϕ denotes the geopotential height. The brackets represent vertical integration. The surface evaporation is represented by E_s. The surface precipitation is represented by Prec. The net downward radiative flux is represented by R; the subscripts TOA and SRF represent the top of the atmosphere and the surface, respectively. The latent heat is represented by L_v; SH is the surface sensible heat flux; and $\boldsymbol{\tau}_s$ denotes the wind stress at the surface. Other variables are as commonly used.

The final analysis is obtained by minimizing the cost function of

$$I(t) = (u-u_o)^{\mathrm{T}}\mathbf{B}_u^{-1}(u-u_o) + (v-v_o)^{\mathrm{T}}\mathbf{B}_v^{-1}(v-v_o) + (s-s_o)^{\mathrm{T}}\mathbf{B}_s^{-1}(s-s_o) + (q-q_o)^{\mathrm{T}}\mathbf{B}_q^{-1}(q-q_o), \tag{24-10}$$

where variables with the subscript o represent the first guess from preprocessed balloon sounding and wind profiler measurements or operational analysis; $\mathbf{B}$ is the error covariance matrix of the state variable.

Terms on the right-hand sides of Eqs. (24-6)–(24-9) are obtained from ARM and satellite measurements at the surface and TOA. Area-averaged precipitation is from radar measurements. Other surface variables are from the suite of stations deployed within a sounding array. These are described in section 6. In some cases, fluxes are derived from statistical interpolation between the limited number of stations and the background fields from the reanalysis products. Since each field experiment has different instrumentation and measurement configurations, the preprocessing of surface and atmospheric measurements is often specific to different experiments, and visual inspections of all input data are necessary.

The minimization of the cost function in Eq. (24-10) requires the specification of the error covariance matrices. These errors are taken as the sum of instruments and measurement biases and sampling biases in Zhang et al. (2001). The instrument and measurement biases are assumed to be $0.5\,\mathrm{m\,s^{-1}}$ for winds, 0.2 K for temperature, and 3% of the specific humidity for water vapor. These were estimated by instrument mentors. The sampling biases are estimated to be 20% of the temporal variances of the fields. In past analyses, the errors are assumed to be independent among different locations and variables. This assumption is being revised to allow for error covariance. Zhang and Lin (1997) described the minimization algorithm of Eq. (24-10).

The final analysis, therefore, is the closest to balloon sounding and wind profiler data or operational analysis that satisfies the required constraints of Eqs. (24-6)–(24-9). The divergence terms in these equation terms are calculated by using the line-integral method. The atmospheric state variables at the boundary stations are preprocessed by using the regular grid method so that data from all profiling stations are used.

The constraining requirements ensure that what enters into the atmospheric column is equal to what exits from the column and at the TOA as well as at the surface after adjusting for column-integrated temporal change. The

forcing data can be considered as a better fitting of the atmospheric analysis to more observational measurements.

The terms on the right-hand side of Eqs. (24-6)–(24-9) are currently treated as known fields. Sensitivities of the analyzed fields to their uncertainties are used to characterize the errors in the forcing data (Zhang et al. 2001). In theory, these constraining variables also can be subject to variational adjustments based on their uncertainties. The imposed constraints can be expanded to include other known physical relationships and measurements, such as clear-sky water vapor and thermodynamic equations and radiance measurements at various wavelengths. The atmospheric state variables should ideally also include cloud hydrometeors, in which case radar reflectivity and cloudy-sky radiance measurements can be used as constraints. Additionally, the error covariance matrices in the cost function should be calculated better. Research is ongoing to make improvements in all these aspects.

6. Input data

The input data for the ARM variational analysis include measurements of both adjustment variables and constraint fields. The adjusted variables are the large-scale state variables: namely, winds, temperature, and humidity. The constraints include surface pressure, surface latent and sensible heat fluxes, wind stress, precipitation, net radiation at the surface and TOA, and column total cloud liquid water. The momentum constraint of Eq. (24-9) was not imposed in the existing analysis because of large sensitivity of the pressure gradient force to errors in temperature, the treatment of which is still under investigation.

The large-scale state variables are obtained primarily from balloonborne sounding measurements. Ideally, high-frequency soundings at least once every 3 h over a well-positioned array are needed to specify the SCM forcing. However, because of logistical difficulties and large expenses of operating coordinated balloon soundings, only during special ARM Intensive Operational Periods (IOPs) were radiosondes launched at 3-hourly or 6-hourly intervals to measure the vertical profiles of winds, temperature, and water vapor mixing ratio.

The majority of these IOPs were conducted at SGP. At the ARM TWP and NSA sites, coordinated balloon sounding measurements are more difficult to make; hence, only one and two IOPs have been conducted at these sites, respectively. ARM also deployed many surface stations at its sites, including various radiometers and surface flux stations. The stations are intended to characterize the water and energy budgets within the domain represented by a GCM grid box. The domain-averaged fluxes also are used in the variational analysis as constraints. The SGP has many more of these surface stations than do the other ARM sites.

At the SGP, hourly profiler measurements of winds are also available at the National Oceanic and Atmospheric Administration (NOAA) wind profiler stations, which are merged with the soundings in the analysis. The SGP site has five ARM sounding stations: the Central Facility (C1) and four boundary facilities (B1, B4, B5, and B6), as well as several NOAA wind profiler sites to provide the needed upper-air measurements (Fig. 24-1a). These boundary sites and wind profilers have not been and are not always available. For the SGP, the variational analysis scheme processes the original upper-air measurements from radiosondes and wind profilers over the analysis grid points (Fig. 24-1a) using the Cressman interpolation scheme (Cressman 1959), which requires a background field from an NWP model's operational analyses. Current variational analysis uses the operational analyses from the NOAA mesoscale model Rapid Update Cycle (RUC) for SGP (Fig. 24-1b) and the ECMWF for other ARM sites. The required constraint variables are derived from measurements of surface observational networks and satellites. Around the ARM SGP site, there is a dense surface network (Fig. 24-1c). The observation platforms include the following:

- Surface meteorological observation system (SMOS) measuring surface precipitation, surface pressure, surface winds, temperature, and relative humidity.
- Energy budget Bowen ratio (EBBR) stations measuring surface latent and sensible heat fluxes and surface broadband net radiative flux.
- Eddy correlation flux measurement system (ECOR) providing in situ averages of the surface vertical fluxes of momentum, sensible heat flux, and latent heat flux.
- Oklahoma and Kansas Mesonet stations (OKM and KAM) measuring surface precipitation, pressure, winds, and temperature.
- Microwave radiometer (MWR) stations measuring the column precipitable water and total cloud liquid water. The stations have experienced changes over the past 20 years, including decommissioning at the ARM boundary facilities.
- Solar and infrared radiation station (SIRS) providing continuous measurements of broadband shortwave (solar) and longwave (atmospheric or infrared) irradiances for downwelling and upwelling components.
- National Weather Service WSR-88D NEXRAD radar and rain gauge providing hourly surface precipitation data to the Arkansas-Red basin River Forecast Center (ABRFC).

The Geostationary Operational Environmental Satellite (GOES) provides satellite measurements, clouds,

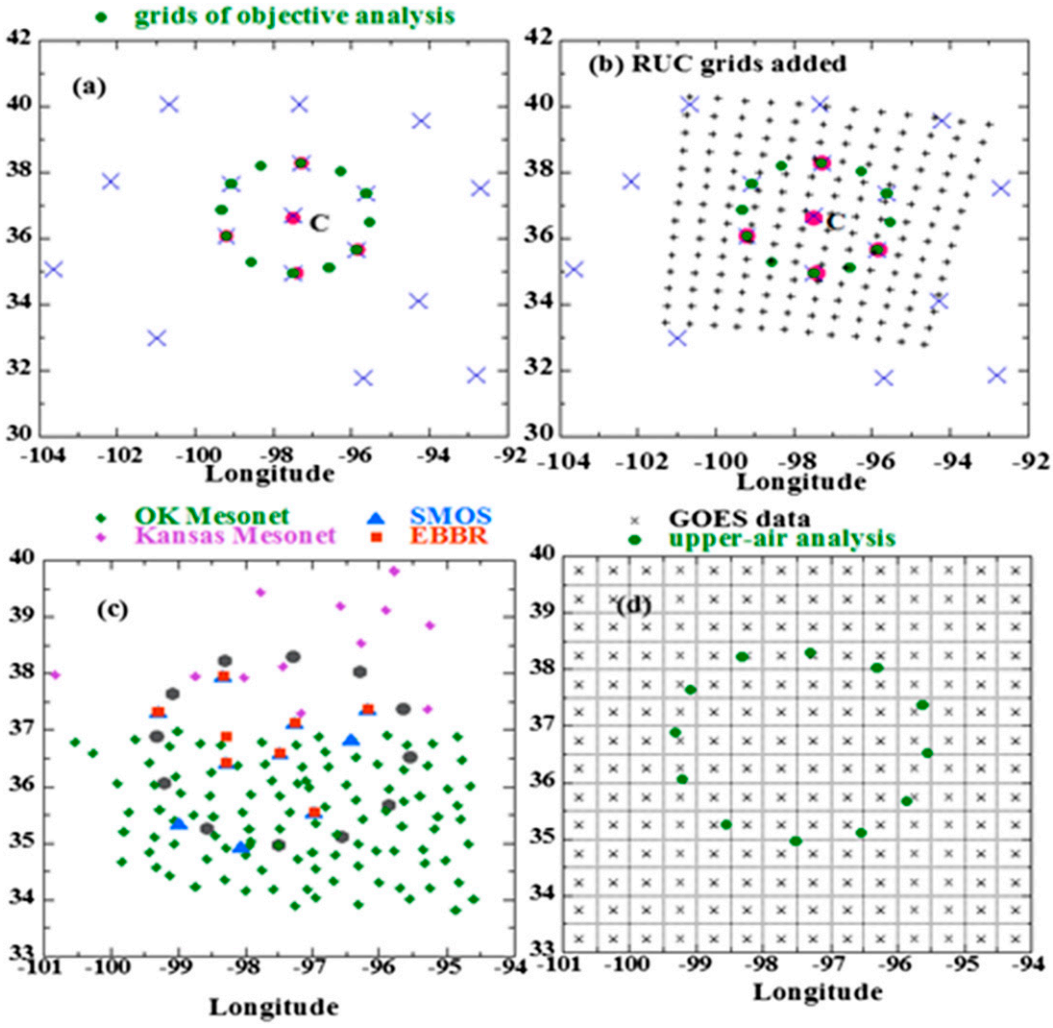

FIG. 24-1. Locations of the ARM upper-air data streams and the analysis grid points at the SGP site in the July 1997 IOP: (a) sounding stations (red circle), wind profilers (blue crosses), and final analysis grids (green circles); (b) RUC grids overlaid on other grids; (c) ARM surface data streams (see text for complete instrument names); and (d) GOES grids over the analysis domain. Adapted from Zhang et al. (2001).

and broadband radiative fluxes at TOA over the 0.5° × 0.5° grids (Fig. 24-1d) (Minnis et al. 1995). All the constraint variables are area-averaged quantities over the analysis domain. To avoid biases of using overcrowding measurement stations in some areas, the algorithm first lays the 0.5° × 0.5° GOES grids over the analysis domain and then derives the required quantities in each small grid box. If there are actual measurements within the subgrid box, simple arithmetic averaging is used to obtain the subgrid box means. Some variables are available from several instruments, as indicated above. They are merged in the arithmetic averaging process. If there is no actual measurement in the small box, the Barnes scheme (Barnes 1964) is used to fill in the missing data. Domain averages of these constraint quantities are obtained by using values from the 0.5° × 0.5° grid boxes within the analysis domain.

To enable SCM research beyond IOPs with coordinated balloon soundings, ARM also used hourly operational analysis of atmospheric fields as input to the constrained variational analysis to derive the so-called continuous forcing dataset (Xie et al. 2004). The operational analyses were constrained by the observed surface observations from ARM and TOA fields from GOES. The advantage of the continuous forcing is that it can be derived for long periods and over most regions of the globe as long as surface and TOA measurements are available. The use of the observed constraints in the analysis can significantly improve the accuracy of the forcing data derived from NWP analyses (Xie et al.

TABLE 24-1. Available ARM variational analysis forcing datasets. The given months and years are when the forcing data are available.

Location	IOP forcing	Continuous forcing
SGP	Jul 1995, Apr 1997, Jun 1997, Sep 1997, Apr 1998, Jan 1999, Mar 1999, Jul 1999, Mar 2000, Sep 2000, Nov 2000, Nov 2002, May 2003, Jun 2007, Apr 2012	Jan 1999–Jun 2011
TWP Darwin	Jan 2006	Three wet seasons between 2004 and 2007
NSA	Oct 2004	Apr 2008
AMF China	—	Nov 2008
AMF ARM MJO Experiment (AMIE) Gan	—	Nov 2011

2004). This method enabled the derivation of forcing data at ARM sites that lack coordinated high-frequency soundings, such as at the TWP, NSA, and ARM Mobile Facilities (AMFs).

7. Available ARM forcing datasets

The constrained variational analysis method has been applied to routinely derive the large-scale forcing data from ARM measurements for SCM and CRM studies. There are two types of variational analysis forcing data products available for the ARM permanent research sites and AMFs. The first is the IOP forcing, which is derived using sounding data collected during ARM major IOPs. The second is the continuous forcing, which is derived using NWP operational analyses for multiyear continuous periods where sounding measurements are not available. For both types of the forcing datasets, the large-scale state variables are constrained with surface and satellite observations.

Table 24-1 lists the available ARM variational analysis forcing datasets. These forcing datasets can be obtained from the ARM data archive (http://iop.archive.arm.gov/arm-iop/0eval-data/xie/scm-forcing). Over the past two decades, ARM has conducted numerous field campaigns in diverse climate regimes around the world to collect detailed observations of clouds and radiation, as well as related atmospheric variables for climate model evaluation and improvement. The majority of these field campaigns were conducted at the ARM SGP site, probably the largest and most extensive climate research site in the world. Major field campaigns at SGP include the June–July 1997 SCM IOP for midlatitude land convection, the March 2000 cloud IOP for frontal systems, the June 2007 Cloud Land Surface Interaction Campaign (CLASIC), and the April–May 2011 Midlatitude Continental Convective Clouds Experiment (MC3E). At the ARM NSA site, ARM conducted the Mixed-Phase Arctic Cloud Experiment (M-PACE) in October 2004 to study mixed-phase clouds and the Indirect and Semi-Direct Aerosol Campaign (ISDAC) in April 2008 to study the aerosol–cloud interaction in the Arctic region. In the tropics, the Tropical Warm Pool–International Cloud Experiment (TWP-ICE) took place in January and February 2006 around the ARM TWP Darwin site to improve understanding of the interaction of tropical convection with its environment. In addition, ARM regularly deploys its AMF in various climate regimes not previously explored. More details about these field campaigns can be found via the ARM website (http://www.arm.gov/campaigns).

The variational analysis forcing data products have been developed for all the major field campaigns conducted at the ARM permanent research sites and some of the AMF deployments. For the SGP and TWP Darwin sites, ARM has also created continuous forcing data over multiple years. These large-scale forcing datasets provide the needed initial and boundary conditions for SCMs and CRMs in studying various observed cloud systems and testing physical parameterizations in climate models.

8. Applications of SCMs and ARM data to understanding and improving models

It is now well recognized in the GCM and NWP communities that SCMs are tools that have a valuable role to play in testing and improving parameterizations by evaluating them empirically against field observations. Early surveys of SCM research have been published by Randall et al. (1996) and Somerville (2000). Since then, many papers have been published by using SCMs and ARM forcing data.

Most of these studies contribute to model improvements in one of the following three ways. The first is the evaluation of the performances of physical parameterizations in operational and global climate models (e.g., Yang et al. 2006; Kennedy et al. 2011; Song et al. 2013). The second is the validation, improvement, and development of parameterizations, including the triggering

and closure assumptions of convection parameterizations (e.g., Xie and Zhang 2000; Zhang 2003; Guichard et al. 2004; Petch et al. 2007); cloud macrophysical schemes (e.g., Zhang et al. 2003); the mass flux parameterization of deep convection (Wu et al. 2009); the parameterization of shallow convection and boundary layer turbulence (Sušelj et al. 2012); and the parameterization of vertical velocity in shallow convection (Wang and Zhang 2014), among others. The third is to use SCMs with ARM forcing data to improve understanding of processes, including growth of ice particles (Comstock et al. 2008), cloud feedbacks (Del Genio et al. 2005), the interaction of deep and shallow convections (Wang and Zhang 2013), and land–atmosphere interactions (Sud et al. 2001). It should be noted that model development and improvement using SCMs is often done in conjunction with CRM or LES simulations under the same large-scale forcing.

Several ARM SCM case studies have been organized, with multiauthored publications. The first case used data from the ARM June 1995 SGP IOP (Ghan et al. 2000). SCMs and CRMs were used to simulate summertime continental convection. This case study settled the subsequent methods of how SCMs are run using observationally derived forcing data. Main results from the paper include the relative superior performance of the CRMs to SCMs, thus justifying the use of CRM results to improve SCMs.

The second ARM SCM case study by Xie et al. (2002) used the summer 1997 SGP IOP as a follow-up of Ghan et al. (2000). It was shown that deficiencies in convective triggering mechanisms were one of the major reasons for model biases. Using a triggering mechanism based solely on the vertical integral of parcel buoyant energy results in overactive convection, which in turn leads to large systematic warm/dry biases in the troposphere. It is also shown that a nonpenetrative convection scheme can underestimate the depth of instability for midlatitude convection, which leads to large systematic cold/moist biases in the troposphere. All models significantly underestimate the surface stratiform precipitation.

The third ARM SCM case study was published by Guichard et al. (2004) using an idealization of ARM June 1997 measurements to evaluate the simulation of deep convection. They found that the SCMs tend to simulate the onset of convection too early, while CRMs tend to simulate the onset too late.

The fourth ARM SCM case study was led by Xie et al. (2005) who used the ARM March 2000 SGP cloud IOP to investigate the parameterizations of frontal clouds. Most SCMs were found to underestimate cloud water and to contain huge biases in cloud ice of both signs. The SCMs underestimated the amount of midlevel clouds, which also appeared in CRMs. They attributed some of these biases to the lack of subgrid-scale dynamical forcing.

A case study for M-PACE was reported by Morrison et al. (2009). They showed that, for single-layer clouds, the simulated ice water path is generally consistent with observed values, and the median SCM and CRM liquid water path is a factor of 3 smaller than observed. For multilevel clouds, however, the models generally overestimate liquid water path and strongly underestimate ice water path. Models with more sophisticated, two-moment treatment of cloud microphysics were found to produce a somewhat smaller liquid water path closer to observations.

The case study for TWP-ICE has been reported in the work of Fridlind et al. (2012), who used CRMs with ARM forcing data. SCM intercomparison results have been reported in Davies et al. (2013) and Petch et al. (2014). All these studies showed how the ice microphysical parameterizations impact the simulated ice contents.

These cases serve as test beds for new parameterizations and as benchmarks for future studies. They are typically accompanied with comprehensive observational datasets that are processed and documented for models. Many other SCM studies by individual investigators have used ARM data. The ones listed in this chapter are a sample of them.

As the ARM Program evolves to have new measurement capabilities and new datasets (Mather and Voyles 2013), more future cases are expected that will target specific processes or scientific problems. An example is the recent case for the Routine ARM Aerial Facility Clouds with Low Optical Water Depths (CLOWD) Optical Radiative Observations (RACORO) campaign (e.g., Vogelmann et al. 2015; Lin et al. 2015).

9. Discussion

It is important to point out some of the limitations in using SCMs with prescribed forcing. First, because the large-scale vertical velocity is prescribed, the simulated precipitation is not the most appropriate field to use to evaluate model physics, as the SCM results are better suited to evaluate fields such as temperature, water vapor, clouds, and radiation. Second, in the case of propagating deep convections or middle-latitude cyclones with differential advection, SCMs should be viewed only as a way to describe a constrained balance of the model physics with the prescribed large-scale condition with possibly little insights on how the model physics are initiated. Third, SCMs cannot capture the interaction of model physics with large-scale dynamics. Some recent studies have attempted to overcome this limitation for tropical convective regimes where weak temperature gradient can

be used to approximately parameterize the vertical velocity with dynamic heating in the SCMs (e.g., Sobel et al. 2001; Kuang 2012). Finally, results from SCMs are not necessarily transferable to global models because of the lack of feedbacks between physics and dynamics.

SCM (and CRM/LES) output is typically very sensitive to the imposed large-scale forcing. In some cases, given the nonlinear behavior of some parameterizations, a small change in the initial condition or forcing can cause the model to drift to a completely different state (Hack and Pedretti 2000). Given the inevitable uncertainties in the forcing data and initial conditions, one strategy is to use ensemble forcing data (Hume and Jakob 2005). Research is ongoing to develop ensemble forcing data that incorporate various uncertainties in the ARM variational algorithm.

Regardless of these limitations, however, many researchers have used SCMs to gain insights on physical parameterizations because they provide a convenient test of models and allow researchers to compare model results with observations and CRM/LES simulations. Results from the SCMs have motivated and led to many updates and modifications to the parameterizations in the current generation of global climate models. With the insights from SCMs, hypotheses and improvements can first be tested in SCMs, then evaluated against CRMs/LESs/observations and tested/implemented in global models.

Acknowledgments. The authors wish to thank the two reviewers and the editors, who provided detailed constructive comments that led to great improvements to an earlier version of this chapter.

REFERENCES

Barnes, S. L., 1964: A technique for maximizing details in numerical weather map analysis. *J. Appl. Meteor.*, **3**, 396–409, doi:10.1175/1520-0450(1964)003<0396:ATFMDI>2.0.CO;2.

Bechtold, P., S. K. Krueger, W. S. Lewellen, E. van Meijgaard, C. H. Moeng, D. A. Randall, A. van Ulden, and S. Wang, 1996: Modeling a stratocumulus-topped PBL: Intercomparison among different one-dimensional codes and with large-eddy simulation. *Bull. Amer. Meteor. Soc.*, **77**, 2033–2042, doi:10.1175/1520-0477(1996)077<2033:MASTPI>2.0.CO;2.

Betts, A. K., and M. J. Miller, 1986: A new convective adjustment scheme. Part II: Single column tests using GATE wave, BOMEX, ATEX, and arctic air mass data sets. *Quart. J. Roy. Meteor. Soc.*, **112**, 693–709, doi:10.1002/qj.49711247308.

Bretherton, C. S., S. K. Krueger, M. C. Wyant, P. Bechtold, E. van Meijgaard, B. Stevens, and J. Teixeira, 1999a: A GCSS boundary-layer cloud model intercomparison study of the first ASTEX Lagrangian experiment. *Bound.-Layer Meteor.*, **93**, 341–380, doi:10.1023/A:1002005429969.

——, and Coauthors, 1999b: An intercomparison of radiatively driven entrainment and turbulence in a smoke cloud, as simulated by different numerical models. *Quart. J. Roy. Meteor. Soc.*, **125**, 391–423, doi:10.1002/qj.49712555402.

Cess, R. D., and Coauthors, 1990: Intercomparison and interpretation of climate feedback processes in 19 atmospheric general circulation models. *J. Geophys. Res.*, **95**, 16 601–16 615, doi:10.1029/JD095iD10p16601.

Comstock, J. M., R.-F. Lin, D. O'C. Starr, and P. Yang, 2008: Understanding ice supersaturation, particle growth, and number concentration in cirrus clouds. *J. Geophys. Res.*, **113**, D23211, doi:10.1029/2008JD010332.

Cressman, G. P., 1959: An operational objective analysis scheme. *Mon. Wea. Rev.*, **87**, 367–374, doi:10.1175/1520-0493(1959)087<0367:AOOAS>2.0.CO;2.

Davies, L., and Coauthors, 2013: A single-column model ensemble approach applied to the TWP-ICE experiment. *J. Geophys. Res.*, **118**, 6544–6563, doi:10.1002/jgrd.50450.

Davies-Jones, R. P., 1993: Useful formulas for computing divergence, vorticity, and their errors from three or more stations. *Mon. Wea. Rev.*, **121**, 713–725, doi:10.1175/1520-0493(1993)121<0713:UFFCDV>2.0.CO;2.

Del Genio, A. D., A. Wolf, and M.-S. Yao, 2005: Evaluation of regional cloud feedbacks using single-column models. *J. Geophys. Res.*, **110**, D15S13, doi:10.1029/2004JD005011.

Ellingson, R. G., J. Ellis, and S. Fels, 1991: The intercomparison of radiation codes used in climate models: Long wave results. *J. Geophys. Res.*, **96**, 8929–8953, doi:10.1029/90JD01450.

Frank, W. M., H. Wang, and J. L. McBridge, 1996: Rawinsonde budget analyses during TOGA COARE IOP. *J. Atmos. Sci.*, **53**, 1761–1780, doi:10.1175/1520-0469(1996)053<1761:RBADTT>2.0.CO;2.

Fridlind, A. M., and Coauthors, 2012: A comparison of TWP-ICE observational data with cloud-resolving model results. *J. Geophys. Res.*, **117**, D05204, doi:10.1029/2011JD016595.

Ghan, S. J., and Coauthors, 2000: A comparison of single column model simulations of summertime midlatitude continental convection. *J. Geophys. Res.*, **105**, 2091–2124, doi:10.1029/1999JD900971.

Gregory, D., and P. R. Rowntree, 1990: A mass flux convection scheme with representation of cloud ensemble characteristics and stability-dependent closure. *Mon. Wea. Rev.*, **118**, 1483–1506, doi:10.1175/1520-0493(1990)118<1483:AMFCSW>2.0.CO;2.

Guichard, F., and Coauthors, 2004: Modelling the diurnal cycle of deep precipitating convection over land with cloud-resolving models and single-column models. *Quart. J. Roy. Meteor. Soc.*, **130**, 3139–3172, doi:10.1256/qj.03.145.

Hack, J. J., and J. A. Pedretti, 2000: Assessment of solution uncertainties in single-column modeling frameworks. *J. Climate*, **13**, 352–365, doi:10.1175/1520-0442(2000)013<0352:AOSUIS>2.0.CO;2.

Hume, T., and C. Jakob, 2005: Ensemble single column modeling (ESCM) in the tropical western Pacific: Forcing data sets and uncertainty analysis. *J. Geophys. Res.*, **110**, D13109, doi:10.1029/2004JD005704.

Iacobellis, S., and R. C. J. Somerville, 1991a: Diagnostic modeling of the Indian monsoon onset. Part I: Model description and validation. *J. Atmos. Sci.*, **48**, 1948–1959, doi:10.1175/1520-0469(1991)048<1948:DMOTIM>2.0.CO;2.

——, and ——, 1991b: Diagnostic modeling of the Indian monsoon onset. Part II: Budget and sensitivity studies. *J. Atmos. Sci.*, **48**, 1960–1971, doi:10.1175/1520-0469(1991)048<1960:DMOTIM>2.0.CO;2.

Kennedy, A. D., D. Xiquan, X. Baike, X. Shaocheng, Z. Yunyan, and C. Junye, 2011: A comparison of MERRA and NARR reanalyses with the DOE ARM SGP data. *J. Climate*, **24**, 4541–4557, doi:10.1175/2011JCLI3978.1.

Kuang, Z., 2012: Weakly forced mock-Walker cells. *J. Atmos. Sci.*, **69**, 2759–2786, doi:10.1175/JAS-D-11-0307.1.

Lane, D. E., R. C. J. Somerville, and S. F. Iacobellis, 2000: Sensitivity of cloud and radiation parameterizations to changes in vertical resolution. *J. Climate*, **13**, 915–922, doi:10.1175/1520-0442(2000)013<0915:SOCARP>2.0.CO;2.

Lee, W.-H., S. F. Iacobellis, and R. C. J. Somerville, 1997: Cloud radiation forcings and feedbacks: General circulation model tests and observational validation. *J. Climate*, **10**, 2479–2496, doi:10.1175/1520-0442(1997)010<2479:CRFAFG>2.0.CO;2.

Lenderink, G., and Coauthors, 2004: The diurnal cycle of shallow cumulus clouds over land: A single-column model intercomparison study. *Quart. J. Roy. Meteor. Soc.*, **130**, 3339–3364, doi:10.1256/qj.03.122.

Lin, W., and Coauthors, 2015: RACORO continental boundary layer cloud investigations. Part III: Separation of parameterization biases in single-column model CAM5 simulations of shallow cumulus. *J. Geophys. Res.*, **120**, 6015–6033, doi:10.1002/2014JD022524.

Lin, X., and R. H. Johnson, 1996: Kinematic and thermodynamic characteristics of the flow over the western Pacific warm pool during TOGA COARE. *J. Atmos. Sci.*, **53**, 695–715, doi:10.1175/1520-0469(1996)053<0695:KATCOT>2.0.CO;2.

Lord, S. J., 1982: Interaction of a cumulus cloud ensemble with the large-scale environment. Part III: Semi-prognostic test of the Arakawa–Schubert cumulus parameterization. *J. Atmos. Sci.*, **39**, 88–103, doi:10.1175/1520-0469(1982)039<0088:IOACCE>2.0.CO;2.

Mather, J. H., and J. W. Voyles, 2013: The ARM Climate Research Facility: A review of structure and capabilities. *Bull. Amer. Meteor. Soc.*, **94**, 377–392, doi:10.1175/BAMS-D-11-00218.1.

Minnis, P., W. L. Smith Jr., D. P. Garber, J. K. Ayers, and D. R. Doelling, 1995: Cloud properties derived from GOES-7 for spring 1994 ARM Intensive Observing Period using version 1.0.0 of the ARM Satellite Data Analysis Program. NASA Reference Publication 1366, 59 pp. [Available online at http://ntrs.nasa.gov/archive/nasa/casi.ntrs.nasa.gov/19960021096.pdf.]

Morrison, H., and Coauthors, 2009: Intercomparison of model simulations of mixed-phase clouds observed during the ARM Mixed-Phase Arctic Cloud Experiment. II: Multilayer cloud. *Quart. J. Roy. Meteor. Soc.*, **135**, 1003–1019, doi:10.1002/qj.415.

Ooyama, K., 1987: Scale-controlled objective analysis. *Mon. Wea. Rev.*, **115**, 2479–2506, doi:10.1175/1520-0493(1987)115<2479:SCOA>2.0.CO;2.

Petch, J. C., M. Willett, R. Y. Wong, and S. J. Woolnough, 2007: Modelling suppressed and active convection. Comparing a numerical weather prediction, cloud-resolving and single-column model. *Quart. J. Roy. Meteor. Soc.*, **133**, 1087–1100, doi:10.1002/qj.109.

——, A. Hill, L. Davies, A. Fridlind, C. Jakob, Y. Lin, S. Xie, and P. Zhu, 2014: Evaluation of intercomparisons of four different types of model simulating TWP-ICE. *Quart. J. Roy. Meteor. Soc.*, **140**, 826–837, doi:10.1002/qj.2192.

Ramanathan, V., and J. A. Coakley Jr., 1978: Climate modeling through radiative–convective models. *Rev. Geophys.*, **16**, 465–489, doi:10.1029/RG016i004p00465.

Randall, D. A., and D. G. Cripe, 1999: Alternative methods for specification of observed forcing in single-column models and cloud system models. *J. Geophys. Res.*, **104**, 24 527–24 545, doi:10.1029/1999JD900765.

——, K.-M. Xu, R. C. J. Somerville, and S. Iacobellis, 1996: Single-column models and cloud ensemble models as links between observations and climate models. *J. Climate*, **9**, 1683–1697, doi:10.1175/1520-0442(1996)009<1683:SCMACE>2.0.CO;2.

Sobel, A. H., J. Nilsson, and L. M. Polvani, 2001: The weak temperature gradient approximation and balanced tropical moisture waves. *J. Atmos. Sci.*, **58**, 3650–3665, doi:10.1175/1520-0469(2001)058<3650:TWTGAA>2.0.CO;2.

Somerville, R. C. J., 2000: Using single-column models to improve cloud-radiation parameterizations. *General Circulation Model Development: Past, Present, and Future*. International Geophysics Series, Vol. 40, Academic Press, 641–657.

Song, H., W. Lin, Y. Lin, A. B. Wolf, R. Neggers, L. J. Donner, A. D. Del Genio, and Y. Liu, 2013: Evaluation of precipitation by seven SCMs against ARM observations at the SGP site. *J. Climate*, **26**, doi:10.1175/JCLI-D-12-00263.1.

Stokes, G. M., and S. E. Schwartz, 1994: The Atmospheric Radiation Measurement (ARM) Program: Programmatic background and design of the cloud and radiation test bed. *Bull. Amer. Meteor. Soc.*, **75**, 1201–1221, doi:10.1175/1520-0477(1994)075<1201:TARMPP>2.0.CO;2.

Sud, Y. C., D. M. Mocko, G. K. Walker, and R. D. Koster, 2001: Influence of land surface fluxes on precipitation: Inferences from simulations forced with four ARM-CART SCM datasets. *J. Climate*, **14**, 3666–3691, doi:10.1175/1520-0442(2001)014<3666:IOLSFO>2.0.CO;2.

Sušelj, K., J. Teixeira, and G. Matheou, 2012: Eddy diffusivity/mass flux and shallow cumulus boundary layer: An updraft PDF multiple mass flux scheme. *J. Atmos. Sci.*, **69**, 1513–1533, doi:10.1175/JAS-D-11-090.1.

Thompson, R. M., S. W. Payne, E. E. Recker, and R. J. Reed, 1979: Structure and properties of synoptic-scale wave disturbances in the intertropical convergence zone of the eastern Atlantic. *J. Atmos. Sci.*, **36**, 53–72, doi:10.1175/1520-0469(1979)036<0053:SAPOSS>2.0.CO;2.

Vogelmann, A., and Coauthors, 2015: RACORO continental boundary layer cloud processes: 1. Case study generation and ensemble large-scale forcings. *J. Geophys. Res. Atmos.*, **120**, 5962–5992, doi:10.1002/2014JD022713.

Wang, X., and M. Zhang, 2013: An analysis of parameterization interactions and sensitivity of single-column model simulations to convection schemes in CAM4 and CAM5. *J. Geophys. Res. Atmos.*, **118**, 8869–8880, doi:10.1002/jgrd.50690.

——, and ——, 2014: Vertical velocity in shallow convection for different plume types. *J. Adv. Model. Earth Syst.*, **6**, 478–489, doi:10.1002/2014MS000318.

Wu, J., A. D. Del Genio, M.-S. Yao, and A. B. Wolf, 2009: WRF and GISS SCM simulations of convective updraft properties during TWP-ICE. *J. Geophys. Res.*, **114**, D04206, doi:10.1029/2008JD010851.

Xie, S., and M. H. Zhang, 2000: Impact of the convective triggering function on single-column model simulations. *J. Geophys. Res.*, **105**, 14 983–14 996, doi:10.1029/2000JD900170.

——, and Coauthors, 2002: Intercomparison and evaluation of cumulus parameterizations under summertime midlatitude continental conditions. *Quart. J. Roy. Meteor. Soc.*, **128**, 1095–1136, doi:10.1256/003590002320373229.

——, R. T. Cederwall, M. Zhang, and J. J. Yio, 2003: Comparison of SCM and CSRM forcing data derived from the ECMWF model and from objective analysis at the ARM

SGP site. *J. Geophys. Res.*, **108**, 4499, doi:10.1029/2003JD003541.

——, ——, and ——, 2004: Developing long-term single-column model/cloud system–resolving model forcing data using numerical weather prediction products constrained by surface and top of the atmosphere observations. *J. Geophys. Res.*, **109**, D01104, doi:10.1029/2003JD004045.

——, and Coauthors, 2005: Simulations of midlatitude frontal clouds by single-column and cloud-resolving models during the Atmospheric Radiation Measurement March 2000 cloud intensive operational period. *J. Geophys. Res.*, **110**, D15S03, doi:10.1029/2004JD005119.

——, S. A. Klein, J. J. Yio, A. C. M. Beljaars, C. N. Long, and M. Zhang, 2006: An assessment of ECMWF analyses and model forecasts over the North Slope of Alaska using observations from the ARM Mixed-Phase Arctic Cloud Experiment. *J. Geophys. Res.*, **111**, D05107, doi:10.1029/2005JD006509.

Yang, F. A., H. B. Pan, S. C. Krueger, S. D. Moorthi, and S. E. Lord, 2006: Evaluation of the NCAP Global Forecast System at the ARM SGP site. *Mon. Wea. Rev.*, **134**, 3668–3690, doi:10.1175/MWR3264.1.

Zhang, G. J., 2003: Convective quasi-equilibrium in the tropical western Pacific: Comparison with midlatitude continental environment. *J. Geophys. Res.*, **108**, 4592, doi:10.1029/2003JD003520.

Zhang, M. H., and J. L. Lin, 1997: Constrained variational analysis of sounding data based on column-integrated budgets of mass, heat, moisture and momentum: Approach and application to ARM measurements. *J. Atmos. Sci.*, **54**, 1503–1524, doi:10.1175/1520-0469(1997)054<1503:CVAOSD>2.0.CO;2.

——, ——, R. Cederwall, J. Yio, and S. C. Xie, 2001: Objective analysis of ARM IOP data: Method and sensitivity. *Mon. Wea. Rev.*, **129**, 295–311, doi:10.1175/1520-0493(2001)129<0295:OAOAID>2.0.CO;2.

——, W. Lin, C. Bretherton, J. J. Hack, and P. J. Rasch, 2003: A modified formulation of fractional stratiform condensation rate in the NCAR Community Atmospheric Model (CAM2). *J. Geophys. Res.*, **108**, 4035, doi:10.1029/2002JD002523.

Zhu, P., and Coauthors, 2005: Intercomparison and interpretation of single-column model simulations of a nocturnal stratocumulus-topped marine boundary layer. *Mon. Wea. Rev.*, **133**, 2741–2758, doi:10.1175/MWR2997.1.